Pharm Res (2014) 31:2503–2515
DOI 10.1007/s11095-014-1346-y

RESEARCH PAPER

Delivery of a Monomeric p53 Subdomain with Mitochondrial Targeting Signals from Pro-Apoptotic Bak or Bax

Karina J. Matissek • Abood Okal • Mohanad Mossalam • Carol S. Lim

Received: 12 November 2013 / Accepted: 24 February 2014 / Published online: 15 March 2014

ABSTRACT

Purpose p53 targeted to the mitochondria is the fastest and most direct pathway for executing p53 death signaling. The purpose of this work was to determine if mitochondrial targeting signals (MTSs) from pro-apoptotic Bak and Bax are capable of targeting p53 to the mitochondria and inducing rapid apoptosis.

Methods p53 and its DNA-binding domain (DBD) were fused to MTSs from Bak (p53-BakMTS, DBD-BakMTS) or Bax (p53-BaxMTS, DBD-BaxMTS). Mitochondrial localization was tested via fluorescence microscopy in 1471.1 cells, and apoptosis was detected via 7-AAD in breast (T47D), non-small cell lung (H1373), ovarian (SKOV-3) and cervical (HeLa) cancer cells. To determine that apoptosis is via the intrinsic apoptotic pathway, TMRE and caspase-9 assays were conducted. Finally, the involvement of p53/Bak specific pathway was tested.

Results MTSs from Bak and Bax are capable of targeting p53 to the mitochondria, and p53-BakMTS and p53-BaxMTS cause apoptosis through the intrinsic apoptotic pathway. Additionally, p53-BakMTS, DBD-BakMTS, p53-BaxMTS and DBD-BaxMTS caused apoptosis in T47D, H1373, SKOV-3 and HeLa cells. The apoptotic mechanism of p53-BakMTS and DBD-BakMTS was Bak dependent.

Conclusion Our data demonstrates that p53-BakMTS (or BaxMTS) and DBD-BakMTS (or BaxMTS) cause apoptosis at the mitochondria and can be used as a potential gene therapeutic in cancer.

KEY WORDS apoptosis · Bak · Bax · mitochondria · p53

K. J. Matissek • A. Okal • M. Mossalam • C. S. Lim (✉)
Department of Pharmaceutics and Pharmaceutical Chemistry
University of Utah, Salt Lake City, Utah, USA
e-mail: carol.lim@pharm.utah.edu

K. J. Matissek
Department of Pharmaceutics and Biopharmacy
Philipps-Universität, Marburg, Germany

ABBREVIATIONS

7-AAD	7-Aminoactinomycin D
BakMTS	MTS from Bak
BaxMTS	MTS from Bax
CCO	MTS from cytochrome c oxidase
CS	C-segment
DBD	DNA binding domain
E	Nuclear export signal
MBD	MDM2 binding domain
MDM2	Murine double minute 2
MOMP	Mitochondrial outer membrane permeabilization
MTS	Mitochondrial targeting signal
NLS	Nuclear localization signal
OTC	MTS from ornithine transcarbamylase
PCC	Pearson's correlation coefficient
PRD	Proline-rich domain
TA	Transactivation domain
TD	Tetramerization domain
TM	Transmembrane
TMRE	Tetramethylrhodamine, ethyl ester
TOM	MTS from translocase of the outer membrane (TOM20)
XL	MTS from Bcl-XL

INTRODUCTION

The tumor suppressor p53 exhibits distinct functions at the cytoplasm, the nucleus and the mitochondria (1). Under normal conditions, the E3 ligase murine double minute 2 (MDM2) binds to the MDM2 binding domain (MBD) of p53 prompting polyubiquitination of terminal lysines on the C-terminus of p53, which marks p53 for proteasomal degradation (2). Upon stress induction, such as DNA damage or ER stress, cytoplasmic p53 translocates either to the nucleus (3) or to the mitochondria (4). Three nuclear localization signals (NLS) in the C-terminus of p53 are responsible for p53

nuclear localization (5). In the nucleus, p53 forms a tetramer via its tetramerization domain (TD) (3) allowing its DNA binding domain (DBD) to bind to DNA activating various genes that are involved in apoptosis, DNA repair and cell cycle arrest (1).

Although p53 does not contain a mitochondrial targeting signal (MTS), it can still translocate to the mitochondria. Machenko *et al.* postulated that MDM2 triggers dimer formation and mono-ubiquitination of cytoplasmic p53 resulting in mitochondrial import via herpesvirus-associated ubiquitin-specific protease (6). At the mitochondrial outer membrane, p53 directly interacts with pro-apoptotic (Bak or Bax) (7,8) and anti-apoptotic Bcl-2 family members (Bcl-XL, Bcl-2, Mcl-1, Bcl-w, and A1) (9–11) through a sequential mechanism first binding anti-apoptotic Bcl-2 proteins followed by binding to pro-apoptotic Bak (Fig. 1) or Bax (12). Activation of Bak (Fig. 1) or Bax leads to homotetramer formation, which causes cytochrome c release from the intermembrane space (13). Binding of cytochrome c to APAF-1 stimulates the assembly of a hepameric, wheel-like structure known as the apoptosome (13). The apoptosome activates the initiator caspase-9 which initiates the executioner apoptotic caspase-3 and caspase-7 (Fig. 1) (14). Their proteolytic activity leads to nuclear fragmentation, chromatin condensation and cell shrinking, also known as programed cell death or apoptosis (4).

In cancer cells, overexpression of Bcl-2, Bcl-XL and Mcl-1 correlates with more aggressive phenotypes and leads to chemotherapy resistance (15–17). Many agents have been identified to target the anti-apoptotic Bcl-2 family members such as navitoclax (inhibits Bcl-2, Bcl-XL, and Bcl-w) and ABT-199 (inhibits Bcl-2) (17). These therapeutics initiate apoptosis by neutralizing anti-apoptotic proteins at the mitochondria thus allowing the pro-apoptotic Bcl-2 family members Bak or Bax to homo-oligomerize leading to apoptosis (18). However, these inhibitors do not inactivate anti-apoptotic Mcl-1 (17). Overexpression of Mcl-1 is linked to reduced response to chemotherapy and poor prognosis which limits the therapeutic options for navitoclax and ABT-199 (17). Mcl-1 (and to a certain extent Bcl-XL) is the main inhibitor of Bak (9,19) while Bax is mainly inhibited by Bcl-2 and Bcl-w (20). Our approach is to *directly* activate pro- apoptotic Bak and Bax by targeting p53 to the mitochondria using Bak's or Bax's own MTSs (Fig. 2). Targeting p53 to the mitochondria executes the shortest apoptotic pathway for p53. *wt* p53 mostly translocates to the nucleus due to its NLS, forms a tetramer, binds to DNA, produces mRNA which is then translated to proteins, and after that these proteins need to translocate to their designated compartment. On the other hand mitochondrially targeted p53 directly interacts with pro- and anti- apoptotic proteins at the mitochondria resulting directly in apoptosis.

The MTSs of Bak or Bax are located on the C-terminal hydrophobic regions of these proteins. The C-terminus contains the transmembrane domain (TM) and the C-segment (CS) (21,22). The amino acid sequences of the MTSs are as follows: for Bax, GTPT*WQTVTIFVAGVLTASLTI*WKKMG and for Bak, GNGP*ILNVLVVLGVVLLGQFVV*RRFFKS, with the TM domain in italics and the CS base pairs underlined. The TM inserts both proteins into the mitochondrial outer membrane (tail anchored proteins) with at least two of the basic amino acids in the CS being necessary for the insertion (Fig. 3) (22). Bax, which is in the cytoplasm, sequesters its TM in its hydrophobic surface groove. Once an apoptotic stimuli occurs, the TM gets externalized, targets Bax to the mitochondria, and inserts itself into the mitochondrial outer membrane (Fig. 3) (21,23). However, Bak is always present at the mitochondrial outer membrane sequestered by Mcl-1 (and Bcl-XL) (Figs. 1 and 3) (19).

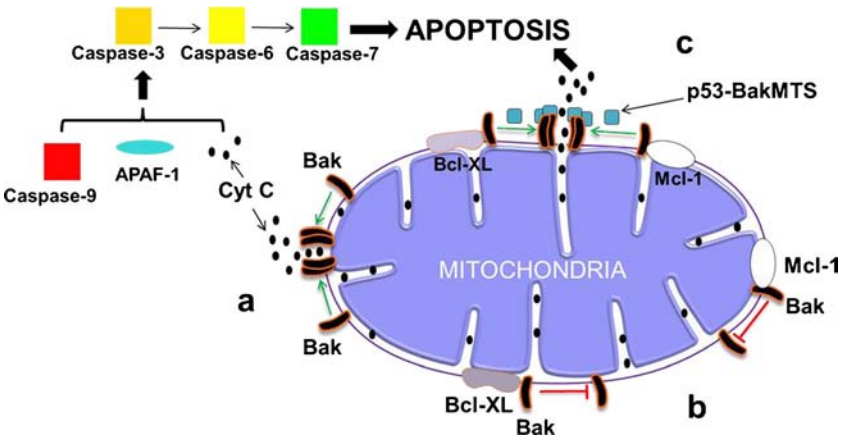

Fig. 1 Intrinsic mitochondrial pathway. (**a**) Upon apoptotic stimuli, Bak homo- oligomerization allows pore formation and cytochrome c release. (**b**) Mcl-1 and Bcl-XL sequester Bak and do not allow homo-oligomerization (**c**) p53-BakMTS binds Bak, releases Bak from both Mcl-1 and Bcl-XL, and allows homo-oligomerization and cytochrome c release which results in apoptosis. On the other hand, Bax is sequestered by Bcl-2 and Bcl-w. p53-BaxMTS binds to Bax, releases Bax from Bcl-2 and Bcl-w and causes apoptosis (pathway for Bax not shown).

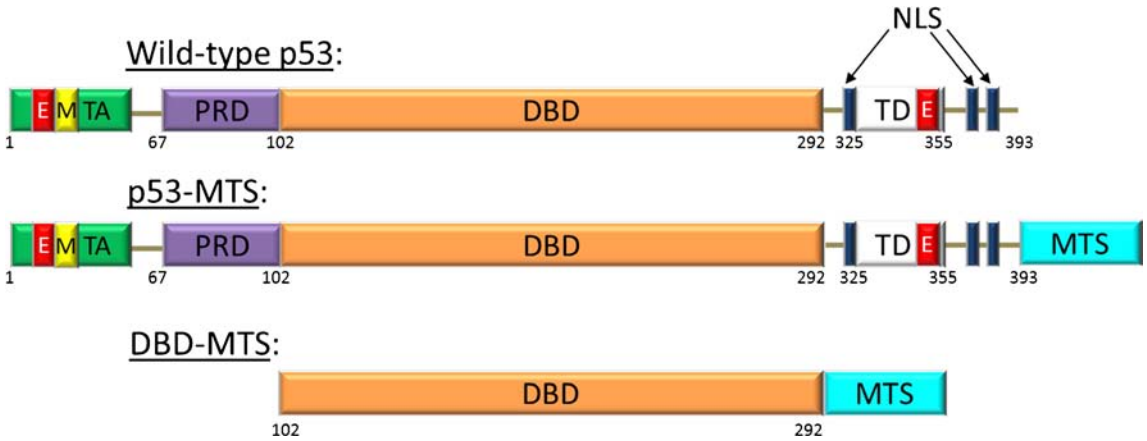

Fig. 2 Schematic representation of experimental constructs: Wild-type p53 is divided into N-terminus, DNA binding domain (DBD) and C-terminal region. The N-terminus consists of a transactivation domain (TA), nuclear export signal (E), MDM2 binding domain (M) and proline-rich domain (PRD). The C-terminus contains three nuclear localization signals (NLS), nuclear export signal (E) and tetramerization domain (TD). p53-MTS wild-type p53 was fused to the mitochondrial targeting signal (MTS) from Bak or Bax. DBD-MTS DNA-binding domain of p53 was fused to the MTS from Bak or Bax.

As mentioned before *wt* p53 does not contain a MTS. Therefore, our approach is to achieve mitochondrial targeting of p53 by fusing the MTSs from Bak or Bax to p53. Murphy and colleagues have reported that *wt* p53 is required to be in a dimeric or tetrameric form in order to activate pro-apoptotic Bak (24). In addition, the DBD has been reported to interact with pro-apoptotic Bak (25) and inhibit anti-apoptotic Bcl-XL (10) and Bcl-2 (11). Here, we show our finding that the DBD in isolation with a MTS from Bak or Bax is sufficient to induce apoptosis in different cancer cells.

MATERIALS AND METHODS

Cell Lines and Transient Transfections

1471.1 murine adenocarcinoma cells (a kind gift of G. Hager, NCI, NIH), T47D human ductal breast epithelial tumor cells (ATCC, Manassas, VA), H1373 human non-small cell lung carcinoma cells (a kind gift from Dr. Andrea Bild, University of Utah), SKOV-3 human ovarian adenocarcinoma cells (a kind gift from Dr. Margit Janat-Amsbury, University of Utah) and HeLa human epithelial cervical adenocarcinoma cells (ATCC) were grown as monolayers in DMEM (1471.1, SKOV-3) or RPMI (T47D, H1373, HeLa) (Invitrogen, Carlsbad, CA) supplemented with 10% FBS (Invitrogen), 1% penicillin-streptomycin (Invitrogen), 1% glutamine (Invitrogen) and 0.1% gentamycin (Invitrogen) and maintained in a 5% CO_2 incubator at 37°C. T47D media was additionally supplemented with 4 mg/L insulin (Sigma, St. Louis, MO). For microscopy 7.5×10^4 cells for 1471.1 cells were seeded in a 2 well live cell chamber. For apoptosis assays 3.0×10^5 cells for T47D, 1.0×10^5 cells for HeLa, 2.0×10^5 for H1373 and SKOV-3 were seeded in 6-well plates (Greiner Bio-One, Monroe, NC). To account for varying cell growth rates, different amounts of cells were plated in live cell chambers and 6-well plates. Following

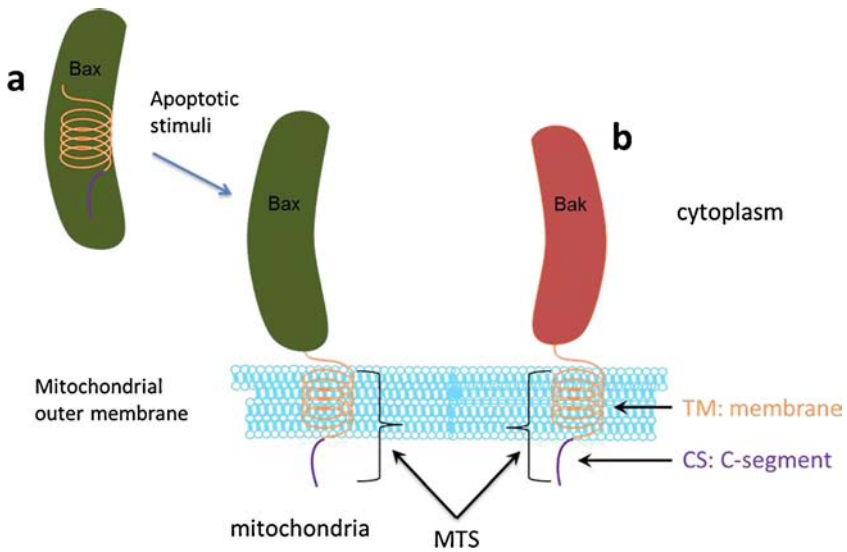

Fig. 3 Bak and Bax insertion into the mitochondria. (**a**) The Bax protein is mainly found in the cytoplasm of healthy cells. Upon apoptotic stimuli, it translocates to the mitochondrial outer membrane. The MTS of the Bax protein, consisting of the transmembrane domain (TM) and the C-segment (CS), becomes exposed for integration into the mitochondrial outer membrane. (**b**) Unlike Bax, Bak is always present at the mitochondrial outer membrane via its TM and CS.

the manufacturer's recommendations 24 h after seeding, transfections were performed using 1 pmol of DNA per well (unless otherwise indicated) and Lipofectamine 2000 (Invitrogen).

Plasmid Construction

pEGFP-p53-BakMTS (p53-BakMTS)

An oligonucleotide encoding the MTS from Bak (5′-GATC CGGCAATGGTCCCATCCTGAACGTGCTGGTGG TTCTGGGTGTGGTTCTGTTGGGCCAGTTTGTG GTACGAAGATTCTTCAAATCATGAG-3′) was annealed to its reverse complementary strand and fused to the C-terminus of EGFP-p53 (26) using the BamHI restriction sites (New England Biolabs, NEB, Ipswich, MA).

pEGFP-BakMTS (E-BakMTS)

The annealed oligonucleotide encoding the MTS from Bak was fused to the C-terminus of EGFP-C1 vector (Clontech, Mountain View, CA) (26) using the BamHI (NEB) restriction sites.

pEGFP-DBD-BakMTS (DBD-BakMTS)

The DNA encoding the DBD was amplified via PCR from previously subcloned pEGFP-p53 (26) using 5′- CCGGGC CCGCGGTCCGGAACCTACCAGGGCAGCTACG-3′ and 5′- CCGGGCCCGCGGGGTACCTTTCTTGCGG AGATTCTCTTCCT and cloned between EGFP and Bak MTS into the multiple cloning site of E-BakMTS using BspEI (NEB) and KpnI (NEB) sites.

pEGFP-p53 K120A, R248A, R273A, R280A, E285A, E287A-Bak (p53m6-BakMTS) and pEGFP-DBD K120A, R248A, R273A, R280A, E285A, E287A-Bak (DBDm6-BakMTS)

K120A, R248A, R273A, R280A, E285A, and E287A mutations were introduced in p53-BakMTS and DBD-BakMTS using the QuickChange II XL Site-Directed Mutagenesis Kit (Agilent, Santa Clara, CA). The primers listed below and their reverse complements were used to introduce the K120A mutation 5′-CATT CTGGGACAGCCGCGTCTGTGACTTGCAC-3′; the R248A mutation 5′- CAGTTCCTGCATGGGCGGCA TGAACGCGAGGCCCATCCT-3′; the R273A mutation 5′-GGGACGGAACAGCTTTGAGGTGGCTGTT TGTGCCTGTCCT-3′; the R280A mutation 5′-TTTG TGCCTGTCCTGGGGCAGACCGGCGCACA-3′; and the E285A, E287A mutations 5′-ACCGGCGCACAGCG GAAGCGAATCTCCGC-3′ (underlined sequence indicate mutation sites).

pEGFP-p53K120E-BakMTS (p53K120E-BakMTS) and pEGFP-DBDK120E-BakMTS (DBDK120E-BakMTS)

The K120E mutation was introduced into p53-BakMTS and DBD-BakMTS via QuickChange II XL Site-Directed Mutagenesis Kit (Agilent) using 5′- GCATTCTGGGACAG CCGAGTCTGTGACTTGCACGTA-3′ and its reverse complement.

pEGFP-p53-BaxMTS (p53-BaxMTS)

An oligonucleotide encoding the MTS from Bax 5′-GATC CTCCTACTTTGGGACGCCCACGTGGCAGACCG TGACCATCTTTGTGG CGGGAGTGCTCACCGCCT CACTCACCATCTGGAAGAAGATGGGCTGAG-3′ was annealed to its reverse complementary strand and fused to the C-terminus of EGFP-p53 (26) using the BamHI (NEB) restriction sites.

pEGFP-BaxMTS (E-BaxMTS)

The annealed oligonucleotide encoding the MTS from Bax was fused to the C-terminus of EGFP-C1 vector (Clontech) (26) using the BamHI (NEB) restriction sites.

pEGFP-DBD-BaxMTS (DBD-BaxMTS)

The DNA encoding the DBD was amplified as mentioned above and cloned between EGFP and BaxMTS into the multiple cloning site of E-Bax using BspEI (NEB) and KpnI (NEB) sites.

Mitochondrial Staining and Microscopy

Prior to microscopy, media in live cell chambers was replaced with media containing 10% charcoal stripped fetal bovine serum (CS-FBS, Invitrogen). To stain the mitochondria, cells were incubated with 150 nM of MitoTracker Red FM (Invitrogen) for 15 min at 37°C and protected from light prior to imaging. All images of 1471.1 and T47D live cells were acquired as previously (26,27) with an Olympus IX71F fluorescence microscope (Scientific Instrument Company, Aurora, CO) with high quality (HQ) narrow band GFP filter (ex, HQ480/20 nm; em, HQ510/20 nm) and HQ:TRITC filter (ex, HQ545/30; em, HQ620/60) from Chroma Technology (Brattleboro, VT) with a 40× PlanApo oil immersion objective (NA 1.00) on an F-View Monochrome CCD camera.

Image Analysis

Images were analyzed by using JACoP plugin in ImageJ software (28). PCC values were generated using Pearson's

correlation coefficient (PCC) with post Costes' automatic threshold algorithm. PCC depends on both the pixel intensity and overlap of signals. A PCC of +1 represents complete colocalization of EGFP constructs with mitochondria; a PCC of −1 represents anti-correlation, and PCC of 0 correlates to random distribution (29). Bolte and Cordelières defined PCC values equal to 0.6 or above to be colocalized (30). For images analysis, experiments were performed three times ($n=3$) with 10 cells analyzed per n and per construct.

7- AAD Assay

Transfected T47D, H1373, SKOV-3 and HeLa cells were pelleted and resuspended in 500 µL PBS (Invitrogen) containing 1 µM 7-aminoactinomycin D (7-AAD) (Invitrogen) for 30 min prior to analysis (26,27). T47D and H1373 cells were analyzed 48 h after transfection, while SKOV-3 and HeLa cells were analyzed 24 h after transfection (time points optimized empirically). Only EGFP positive cells were assayed using the FACS Canto-II (BD- BioSciences, University of Utah Core Facility) with FACS Diva software as previously (26,27). EGFP and 7-AAD were excited at 488 nm, and detected at 507 nm and 660 nm, respectively. Independent transfections of each construct were assayed three times ($n=3$). The highest value (EGFP positive cells stained with 7-AAD) was set at 100%, and the lowest at 0% (relative 7-AAD) as previously (31).

Reporter Gene Assay

3.5 µg of p53-BakMTS, E-BakMTS, p53-BaxMTS, E-BaxMTS, *wt* p53 or EGFP were co-transfected with 3.5 µg of p53-Luc Cis-Reporter (Agilent Technologies) encoding the firefly luciferase gene and 0.35 µg of pRL-SV40 plasmid encoding Renilla luciferase (Promega, Madison, WI) to normalize for transfection efficiency in T47D cells using the Dual-Glo Luciferase assay system as previously (26,31). Luminescence was detected 24 h post transfection using PlateLumino (Stratec Biomedical Systems, Birkenfeld, Germany). Independent transfections of each constructs were assayed three times ($n=3$). The highest value was set at 100% and lowest value (untreated cells) was set as 0% (relative luminescence) as before (26,31).

TMRE Assay

As previously (27), 36 h after transfection T47D cells were incubated with 100 nM tetramethylrhodamine, ethyl ester (TMRE) (Invitrogen) for 30 min at 37°C, pelleted and resuspended in 300 µL annexin-V binding buffer (1×) (Invitrogen). The FACS Canto-II with FACS Diva software was used to analyze only EGFP positive cells (excited at 488 nm with emission 530/35) stained with TMRE (excited at 561 nm laser with the emission 585/15). Loss in TMRE intensity represents mitochondrial depolarization, which correlates with an increase in mitochondrial outer membrane permeabilization (MOMP). Independent transfections of each construct were assayed three times ($n=3$). The highest MOMP value was set as 100% and the lowest as 0% (relative MOMP) as before (27).

Caspase-9 Assay

As previously described (27), 48 h after transfection, T47D cells were tested with SR FLICA Caspase-9 Assay Kit (Immunochemistry Technologies, Bloomington, MN). Cells were incubated with SR FLICA Caspase-9 reagent for 60 min, pelleted and resuspended in 300 µL 1× wash buffer (Immunochemistry Technologies). The FACS Canto-II with FACS Diva software was used to analyzed only EGFP positive cells stained with caspase-9, both were excited with the 488 nm (emission filter 530/35) and the 561 nm laser (emission filter 585/15), respectively. Independent transfections of each construct were assayed three times ($n=3$). The highest value (EGFP positive cells stained with caspase-9) was set as 100% and the lowest as 0% (relative caspase-9) as before (27).

Statistical Analysis

All experiments were done in triplicate ($n=3$). One-way analysis of variance (ANOVA) with Bonferroni's post test was used to determine statistical significance as indicated in figure legend. To determine the degree of colocalization odds ratio with Pearson's Chi-square was applied comparing each PCC value with PCC of 0.6. A p value of <0.6 was considered significant (26,27).

RESULTS

Colocalization of Designed Constructs with the Mitochondria

Since all designed constructs are tagged to EGFP, their mitochondrial localization was determined using fluorescence microscopy in murine adenocarcinoma cells (1471.1). Figure 4a illustrates representative pictures of 1471.1 cells transfected with p53-BakMTS, E-BakMTS, p53-BaxMTS, E-BaxMTS and EGFP. The mitochondrial compartment was stained by MitoTracker red. 1471.1 cells were chosen for the microscopy study because their large size allows for clear distinction between nucleus, cytoplasm and mitochondria. Similar results have been observed for T47D cells (data not shown).

Colocalization of EGFP tagged constructs with the mitochondrial compartment was illustrated by graphing the generated PCC values for each construct as shown in Fig. 4b. PCC values of 0.6 or greater represent colocalization of EGFP

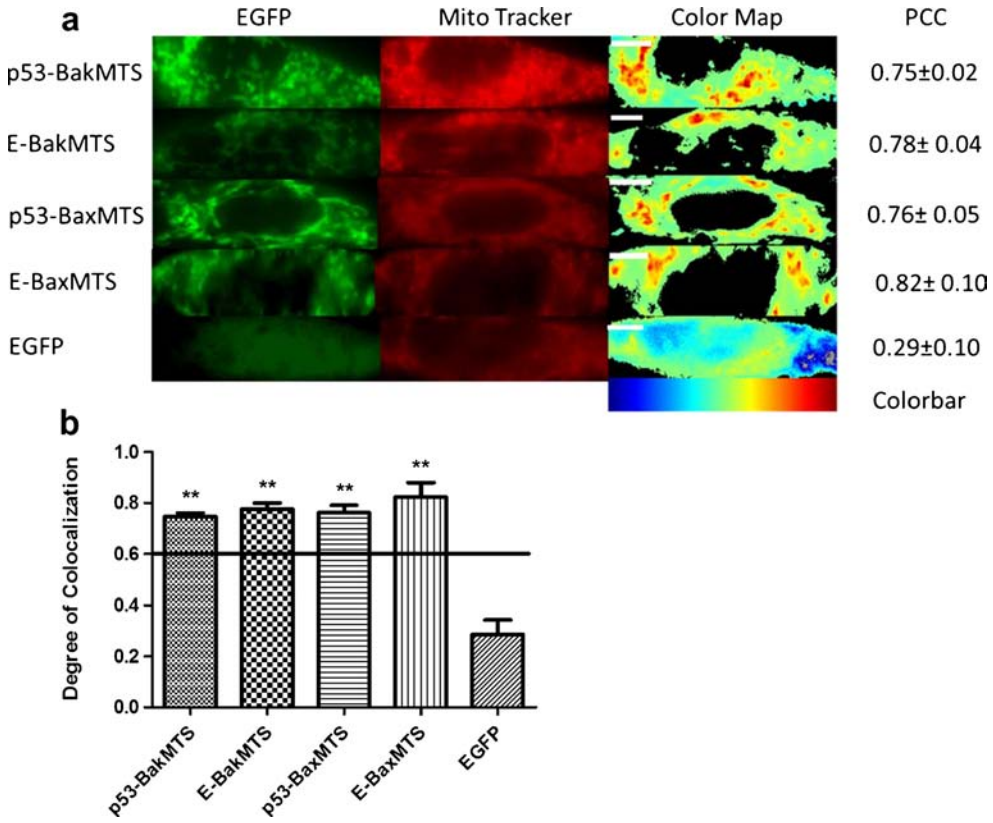

Fig. 4 Mitochondrial localization. (**a**) Representative images of 1471.1 cells transfected with p53-BakMTS, E-BakMTS, p53-BaxMTS, E-BaxMTS and EGFP. *Left* column shows EGFP tagged constructs, middle column mitochondria stained with MitoTracker red and right column depicts colocalization color map. Warm colors (*red*) are considered highly colocalized *versus* cold colors (*blue*) which represent anti-correlation (see colorbars). White scale bars are all 10 μm (**b**) PCC values were graphed for each construct. PCC value equal to 0.6 and above is considered to be colocalized. Statistical analysis was performed using odds ratio with Pearson's Chi-square. The adjusted odds ratio for PCC value of 0.6 was compared with each sample (**$p < 0.01$).

tagged constructs with mitochondria (26–28). p53-BakMTS, E-BakMTS, p53-BaxMTS and E-BaxMTS have a significantly higher PCC value than 0.6. The negative control EGFP shows random distribution (PCC = 0.29) (Fig. 4b). Since *wt* p53 is a transcription factor containing three nuclear localization signals (NLSs) (5), the main fraction of *wt* p53 localizes to the nucleus as we (31) and others (5) have shown before. However, MTSs derived from the pro-apoptotic Bak or Bax protein are capable of overcoming the three NLSs. These Bak and Bax MTSs are capable of targeting EGFP fused to p53 to the mitochondria (Fig. 4).

p53-BakMTS and p53-BaxMTS Induce Late Stage Apoptosis

The ability of p53-BakMTS and p53-BaxMTS to induce apoptosis was tested via 7-AAD assay in T47D breast cancer cells. The 7-AAD dye intercalates into double-stranded DNA of apoptotic/necrotic cells which have a disrupted cell membrane. However, it is not capable of penetrating the intact cell membrane of living cells (32). p53-BakMTS, p53-BaxMTS and *wt* p53 (Fig. 5; compare 1st, 3rd, and 5th bars) show a significant apoptotic effect compared to their corresponding negative controls E-BakMTS, E-BaxMTS and EGFP respectively (Fig. 5; compare 2nd, 4th, and 6th bars).

The apoptotic response induced by p53-BakMTS and p53-BaxMTS is similar to *wt* p53 (Fig. 5; compare 1st, 3rd, and 5th bars). Additionally, MTS negative controls, E-BakMTS and E-BaxMTS, show minimal activity similar to the nontoxic EGFP negative control (Fig 5; compare 2nd, 4th, and 6th bars), which indicates no inherent mitochondrial toxicity for these MTSs by themselves.

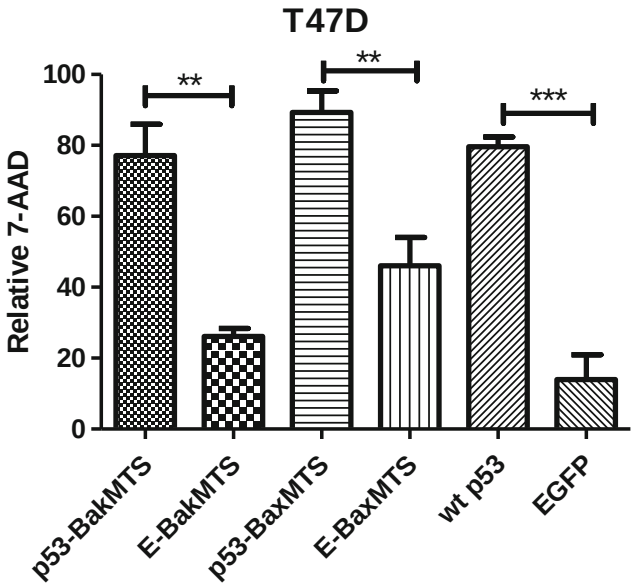

Fig. 5 7-AAD assay in T47D cells, 48 h after transfection. Statistical analysis was performed using one-way ANOVA with Bonferroni's post test; **$p < 0.01$, ***$p < 0.001$. Error bars represent standard deviations from at least three independent experiments ($n = 3$).

p53-BakMTS and p53-BaxMTS Do Not Trigger Apoptosis Through the Nuclear Pathway But Through the Mitochondrial Apoptotic Pathway

To validate that the apoptotic activity of p53-BakMTS and p53-BaxMTS is not due to transcriptional activity at the nucleus, a p53 reporter dual luciferase assay was conducted in T47D cells. The cis reporter system relies on a synthetic promoter which consists of repeats of the transcription recognition consensus for p53 $(TGCCTGGACTTGCCTGG)_{14}$ (33). Nuclear activity was represented as relative luminescence. Endogenous p53 is a nuclear protein and exhibits most of its tumor suppressor functions as a transcription factor. As expected, *wt* p53 shows high transcriptional activity (Fig. 6a; 5th bar). p53-BakMTS, E-BakMTS, p53-BaxMTS, E-BaxMTS (Fig. 6a; compare 1st, 2nd, 3rd, and 4th bars) show no nuclear activity similar to that of the negative control EGFP (Fig. 6a; 6th bar). This suggests that the induction of apoptosis of the mitochondrial constructs p53-BakMTS and p53-BaxMTS seen in Fig. 5 (5th bar) is *not* due to transcriptionally active p53.

To explore if p53-BakMTS and p53-BaxMTS initiate apoptosis through the intrinsic apoptotic pathway, two major hallmarks for the mitochondrial apoptotic pathway (27,34), mitochondrial outer membrane permeabilization (MOMP) and caspase-9 induction, were measured.

The TMRE assay is a direct measurement of MOMP. Homo-oligomerization of Bak or Bax triggers MOMP (7,8) which results in a decrease in mitochondrial membrane potential (35). Cationic dyes such as TMRE accumulate in the mitochondria of healthy cells due to the higher negative charge seen in the mitochondria compared to cytoplasm (27). MOMP results in a loss of TMRE from mitochondria and can be measured via flow cytometry (27). Apoptotic cells are identified by a loss of TMRE fluorescence intensity and are represented as %MOMP induction on the y-axis (Fig. 6b).

The ability of caspase-9 to cleave the peptide sequence leucine-glutamic acid-histidine-aspartic acid determines caspase-9 activity in apoptotic cells (36). When the mitochondrial outer membrane ruptures, cytochrome c is released from the intermembrane space (13). Cytochrome c and Apaf-1 form the apoptosome and activate caspase-9 as shown in

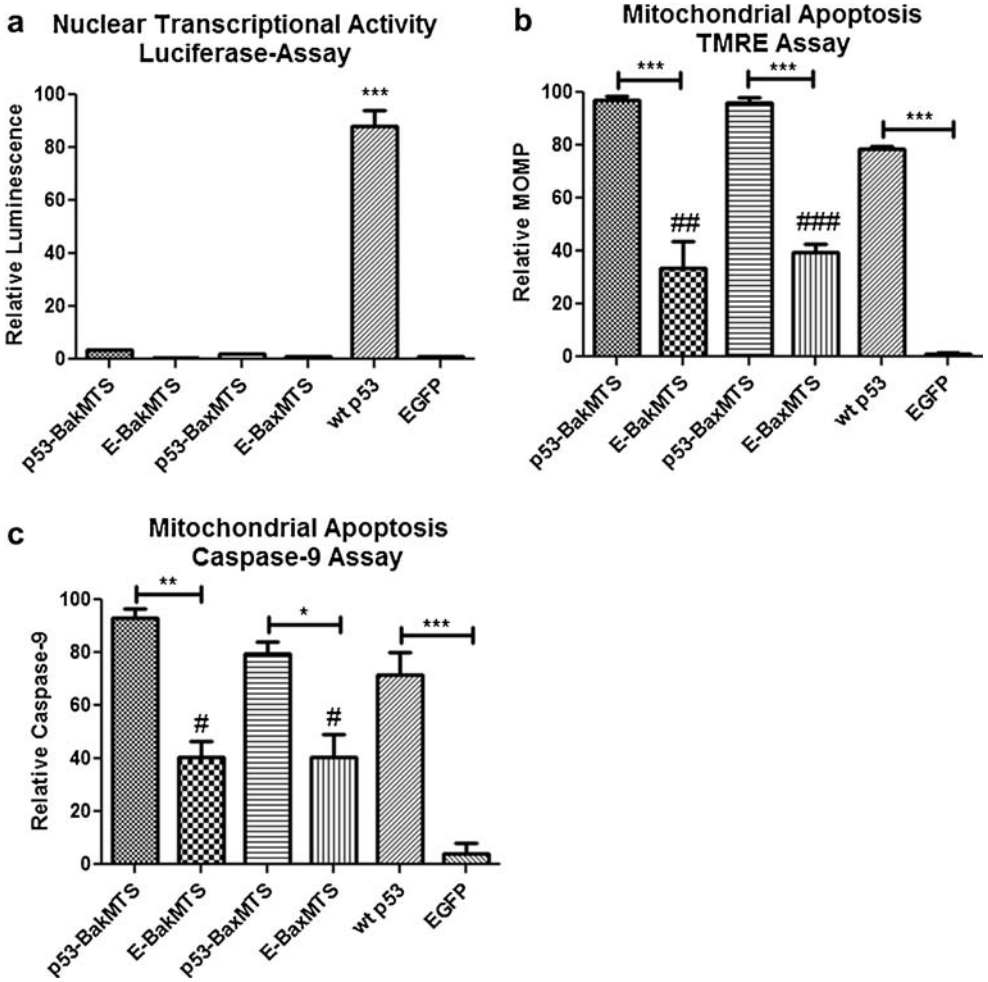

Fig. 6 (**a**) Nuclear transcriptional activity: p53 reporter gene assay: all MTS constructs were tested for their ability to activate p53-Luc Cis-Reporter in T47D cells. *Wt* p53 was used as a positive control and EGFP was considered a negative control. (**b**) Mitochondrial apoptosis: TMRE assay: all constructs were assayed in T47D cells. Mitochondrial depolarization correlates with an increase in MOMP (measured as loss of TMRE fluorescence). (**c**) Mitochondrial apoptosis: Caspase-9 activation was analyzed in T47D cells. All statistical analyses for (**a**), (**b**), and (**c**) were performed by using one-way ANOVA with Bonferroni's post test; $*p < 0.05$, $**p < 0.01$, $***p < 0.001$. Error bars represent standard deviations from at least three independent experiments ($n = 3$). For (**b**) and (**c**) negative controls E-BakMTS and E-BaxMTS were compared to EGFP using one-way ANOVA with Bonferroni's post test; $\#p < 0.05$, $\#\#p < 0.01$, $\#\#\#p < 0.001$. p53-BakMTS and p53-BaxMTS were not significantly higher than *wt* p53.

Fig. 1 (13). Caspase-9 activation was measured via the caspase-9 assay.

p53-BakMTS, p53-BaxMTS and *wt* p53 (Fig. 6b and c; compare 1st, 3rd, and 5th bars) show a significant effect on MOMP and caspase-9 activation compared to their corresponding controls E-BakMTS, E-BaxMTS and EGFP (Fig. 6b and c; compare 2nd, 4rd, and 6th bars). The negative controls E-BakMTS and E-BaxMTS show higher MOMP and caspase-9 activation compared to non-toxic EGFP (Fig. 6b and c; compare 2nd, 4rd, and 6th bars).

DBD-BakMTS and DBD-BaxMTS Induce Late Stage Apoptosis in a Similar Manner as p53-BakMTS and p53-BaxMTS

Pietsch *et al.* showed that p53 must form a dimer or a tetramer to activate Bak oligomerization (24). Additionally, the DBD has been reported to interact with pro-apoptotic Bak (25) and inhibit anti-apoptotic Bcl-XL (10) and Bcl-2 (11). We wanted to test if fusing DBD to MTS from Bak or Bax is sufficient to trigger apoptosis.

Similar levels of 7-AAD positive staining (apoptosis) were detected between cells transfected with DBD-BakMTS compared to p53-BakMTS (Fig. 7a), and cells transfected with DBD-BaxMTS and p53-BaxMTS (Fig. 7b). Additionally, all of these constructs had significantly higher apoptosis compared to cells transfected with MTS negative controls (E-BakMTS, E-BaxMTS) (Fig. 7a and b). DBD fused to Bak or Bax MTS induces a similar apoptotic response as full length p53 fused to these MTSs (Fig. 7a and b).

The Activity of Our Re-engineered Mitochondrially Targeted p53 Constructs in Different Cancer Cell Types

To confirm that the apoptotic potential of our designed constructs causes apoptosis in other cell lines besides T47D breast cancer cells (which express mutant p53 with a L194F point mutation in the DBD of p53) (37), a 7-AAD assay was conducted in non-small cell lung cancer cells (H1373), ovarian cancer cells (SKOV-3) and cervical carcinoma cells (HeLa). H1373 (38) and SKOV-3 cells are p53 null (39) while HeLa cells have endogenous *wt* p53 (40).

In H1373 cells, both p53-BakMTS and DBD-BakMTS apoptotic activities were statistically higher from their negative control E-BakMTS (Fig. 8a; compare 1st, 2nd, and 3rd bars). As expected, *wt* p53 showed significantly higher apoptosis compared to EGFP (Fig. 8a and b; compare 4st, and 5st bars). However, only DBD-BaxMTS activity was significantly higher than E-BaxMTS (Fig. 8b; compare 2nd and 3rd bars) and there was no significant difference between p53-BaxMTS and E-BaxMTS (Fig. 8b; compare 1st and 3rd bars). Additionally, DBD-BakMTS and DBD-BaxMTS had significantly higher activities compared to their positive controls p53-BakMTS and p53-BaxMTS (Fig. 8a and b; compare 1st and 2nd bars).

In SKOV-3 cells, p53-BakMTS and DBD-BakMTS activities were significantly higher than their negative control E-BakMTS (Fig. 8c; compare 1st, 2nd, and 3rd bars). p53-BaxMTS and DBD-BaxMTS activities were only significant when compared to EGFP but no to E-BaxMTS (Fig. 8d; compare 1st, 2nd, 3rd, and 5th bars). The activity of *wt* p53 was similar to nontoxic EGFP in SKOV-3 cells (Fig. 8c and d; compare 4th and 5th bars).

In HeLa cells, p53-BakMTS, DBD-BakMTS (Fig. 8e; compare 1st and 2nd bars), p53-BaxMTS, DBD-BaxMTS (Fig. 8f; compare 1st, and 2nd bars) and *wt* p53 (Fig. 8e and f; 4th bars) apoptotic activities were significant from their corresponding negative controls E-BakMTS (Fig. 8e; 3rd bar), E-BaxMTS (Fig. 8f; 3rd bar) and EGFP (Fig. 8e, and f; 5th bar) respectively. DBD-BakMTS showed a trend of higher apoptotic activity in HeLa cells compared to p53-BakMTS (Fig. 8e; compare 1st and 2nd bars). In addition, DBD-BaxMTS was

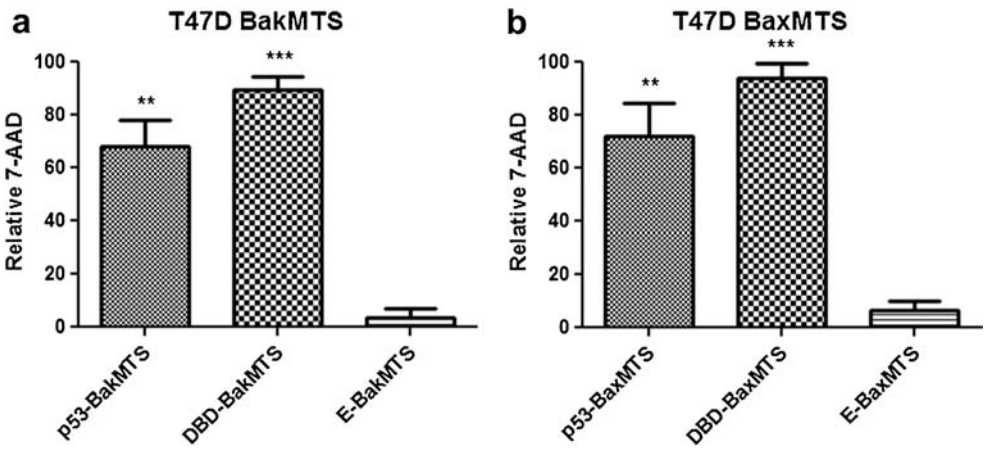

Fig. 7 7-AAD assay in T47D cells: Apoptotic potential of DBD-BakMTS and DBD-BaxMTS were tested. Statistical analysis was performed by using one-way ANOVA with Bonferroni's post test; $^{**}p < 0.01$, $^{***}p < 0.001$ compared to negative controls. Error bars represent standard deviations from at least three independent experiments ($n = 3$).

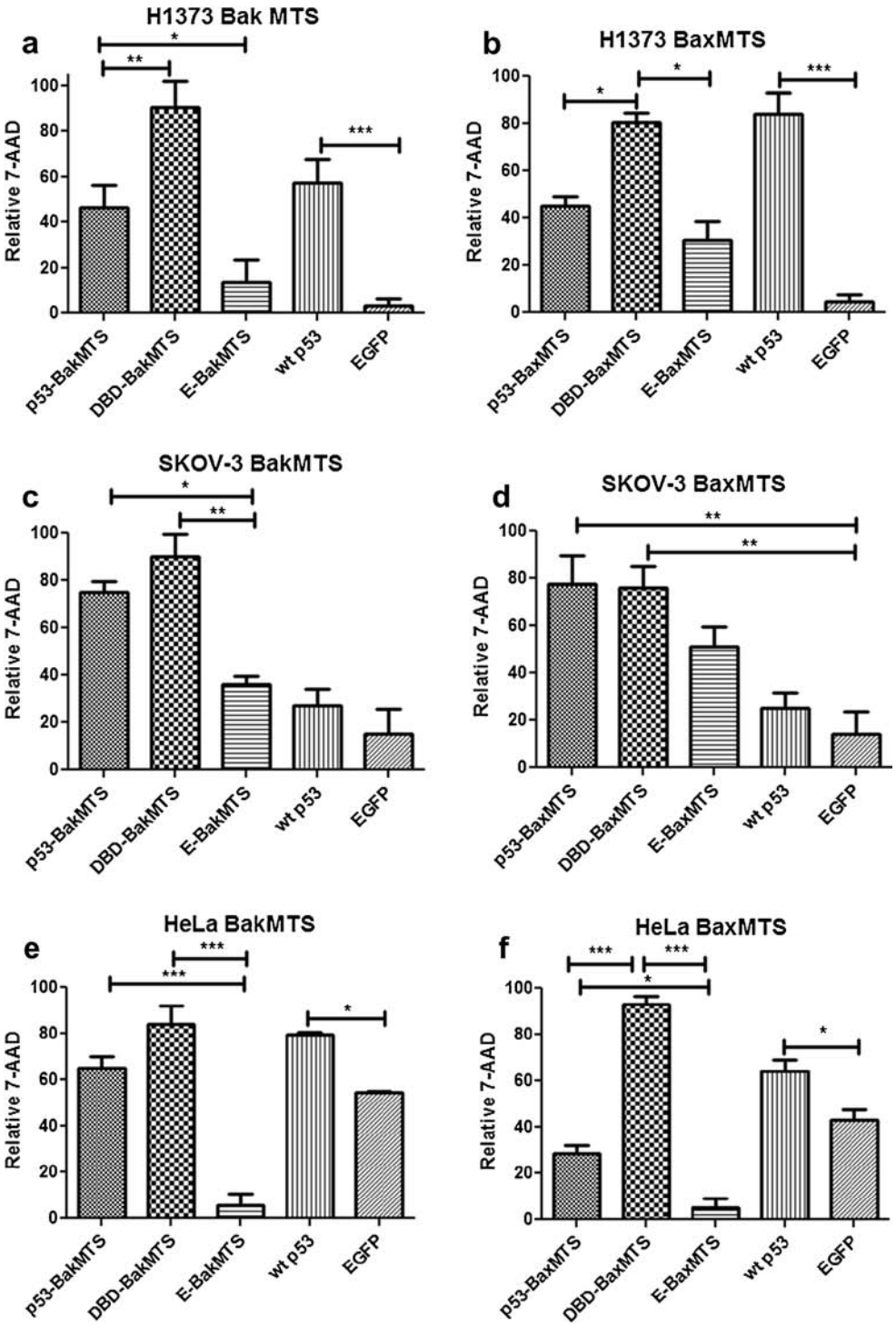

Fig. 8 7-AAD assay was conducted in (**a**) and (**b**) H1373, (**c**) and (**d**) SKOV-3, (**e**) and (**f**) HeLa cells. Statistical analysis was performed by using one-way ANOVA with Bonferroni's post test;*$p < 0.05$, **$p < 0.01$, ***$p < 0.001$. Error bars represent standard deviations from at least three independent experiments ($n = 3$).

significantly higher than p53-BaxMTS (Fig. 8f; compare 1st and 2nd bars).

p53 is known to induce a conformational change in Bax that triggers its oligomerization and mitochondrial permeabilization through a hit-and-run type mechanism (7). However, this p53 interaction with Bax is transient, and the specific interacting residues are not known (7,8,12). On the other hand, it is known that p53 interacts with the Bak protein via amino acids K120, R248, R273, R280, E285 and E287 in p53 (25). Therefore these residues will be mutated to determine if this is a Bak specific interaction. Since p53-BakMTS and DBD-BakMTS showed consistently higher apoptotic activities than their MTS control in all tested cell lines (Figs. 7a and 8a, c and e; compare 1st, 2nd, and 3rd bars), we proceeded to examine the apoptotic mechanism of the Bak MTS constructs.

Exploring the Interaction Between p53-BakMTS, DBD-BakMTS and Pro-apoptotic Bak Protein

It has been reported that p53 interacts with pro-apoptotic Bak protein via amino acids K120, R248, R273, R280, E285 and E287, all of which are found in the DBD of p53 (25). To verify that the apoptotic potential of p53-BakMTS and DBD-BakMTS is through the p53/Bak specific pathway, all sites of p53 (K120A, R248A, R273A, R280A, E285A, E287A) (25) that contact the pro-apoptotic Bak protein were mutated to alanine. The constructs with these six mutations were named p53m6-BakMTS and DBDm6-BakMTS.

Mutating all six of these residues in p53-BakMTS to eliminate binding to pro-apoptotic Bak protein resulted in a complete loss of p53-BakMTS activity (Fig. 9a; 4th bar). p53m6-BakMTS and DBDm6-BakMTS activities are not significantly different from their negative control E-BakMTS suggesting Bak dependent apoptosis (Fig. 9a; compare 3rd, 4th, and 5th bars).

As mentioned above p53 interacts with Bak via its DBD (residues K120, R248, R273, R280, E285, E287). However, p53 also interacts with anti-apoptotic Bcl-XL through the following residues G117, S121, C176, H178, N239, M243, R248, G279, and R280 (10). Therefore, R248 and R280 localized in the DBD of p53 can interact with Bak and Bcl-XL. To exclude any Bcl-XL specific interaction of our designed constructs, only K120 was mutated in the p53-BakMTS and DBD-BakMTS plasmid to glutamic acid. The K120 residue only interacts with Bak not with Bcl-XL (10,25).

Mutating the positively charged lysine 120 to negatively charged glutamic acid (K120E) in p53-BakMTS and DBD-BakMTS resulted in complete loss of apoptotic activity (Fig. 9b; 4th and 5th bars). p53K120E-BakMTS and DBDK120E-BakMTS activities are not statistically significant from the negative control E-BakMTS (Fig. 9b; compare 3rd, 4th, and 5th bars), suggesting a p53/Bak dependent apoptotic mechanism.

DISCUSSION

We and others have shown that targeting p53 to the mitochondria is sufficient to trigger a rapid apoptotic response (4,26,27,41). Previously, our focus was to target p53 to different mitochondrial compartments concluding that targeting it to the outer surface of the mitochondrial membrane is the only compartment that leads to p53-dependent apoptosis (26), rather than non-specific mitochondrial toxicity. So far, only anti-apoptotic binding partners (such as Bcl-XL and Bcl-2) on the outer membrane have been addressed for p53 specific targeting. These constructs sequester anti-apoptotic Bcl-2 family members and therefore *indirectly* activate Bak and Bax (26). Here, our approach is to target p53 directly to Bak and Bax proteins. To our knowledge, this is the first attempt to target p53 to these pro-apoptotic proteins.

Fusing p53 to the MTSs derived from the pro-apoptotic Bak (p53-BakMTS) or Bax (p53-BaxMTS) proteins resulted in localization of these constructs to the mitochondria (Fig. 4) and induction of apoptosis (Figs. 5, 6b and c and 7). The tumor suppressor p53 is a nuclear protein containing three NLSs (5). When targeting p53 to the mitochondria, the chosen MTS must counteract these NLSs. Previously, our lab has targeted p53 with the MTSs from ornithine transcarbamylase (OTC), cytochrome c oxidase (CCO), translocase of the outer membrane (TOM) and Bcl-XL (XL) (26). We have shown that strong MTSs from TOM and XL are capable of overcoming the NLSs in the p53 protein while the weak MTS from CCO and the medium strength MTS from OTC are not strong enough to ensure entire mitochondrial targeting (26). Here, we show that MTSs from Bak and Bax are capable of counteracting the three NLSs in *wt* p53 and can be considered to be strong MTSs (Fig. 4). Additionally, EGFP fused to MTSs from Bak (E-BakMTS) or Bax (E-BaxMTS) showed minimal inherent toxicity which suggests that apoptotic activity of p53-BakMTS and p53-BaxMTS are p53 dependent and not due to MTS toxicity (Fig. 5).

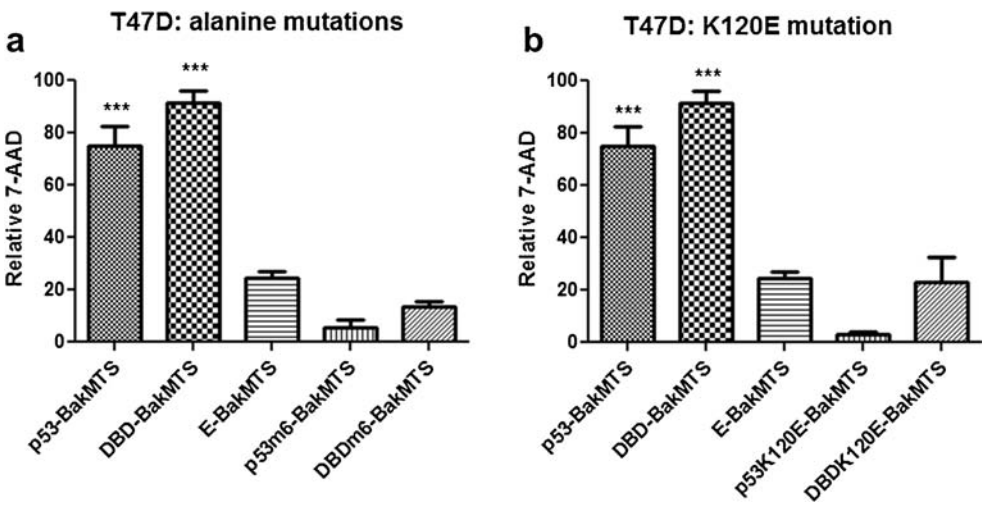

Fig. 9 Decrease in apoptotic potential caused by (**a**) K120A, R248A, R273A, R280A, E285A, E287A (m6) mutations and (**b**) K120E mutation was measured via 7-AAD assay in T47D cells. Statistical analysis was performed by using one-way ANOVA with Bonferroni's post test; $^{**}p < 0.01$, $^{***}p < 0.001$ compared to E-BakMTS. Error bars represent standard deviations from at least three independent experiments ($n = 3$).

Since we confirmed mitochondrial localization and apoptotic potential of p53-BakMTS and p53-BaxMTS, we wanted to examine if the apoptotic response occurs mainly through the mitochondrial pathway or through residual nuclear activity. As expected, *wt* p53 showed high nuclear activity, while p53-BakMTS and p53-BaxMTS showed no transcriptional activity, suggesting that the apoptotic function of p53-BakMTS and p53-BaxMTS is transcriptionally independent (Fig. 6a).

Further, we demonstrated that the apoptotic activity of p53-BakMTS and p53-BaxMTS is through the intrinsic apoptotic pathway. Mitochondrial outer membrane permeabilization (MOMP) and caspase-9 activation can only be initiated via the intrinsic apoptotic pathway (13). In fact, p53-BakMTS and p53-BaxMTS triggered permeabilization of the mitochondrial outer membrane and induced caspase-9 activation confirming the involvement of the intrinsic apoptotic pathway (Fig. 6b and c).

Negative controls E-BakMTS and E-BaxMTS showed some MOMP and caspase-9 activation which was higher than EGFP but still significantly lower than p53-BakMTS and p53-BaxMTS (Fig. 6b and c). However, this is not reflected in the more final apoptosis assay 7-AAD (Fig. 5) (32). It has been reported that cells can recover from mitochondrial outer membrane permeabilization (MOMP) which is measured by TMRE; cells can also recover from caspase-9 activation (13). Therefore, sending GFP to the mitochondria is slightly toxic to the cells reflected by TMRE and caspase-9 assay (Fig. 6) but does not translate into final cell death measured by 7-AAD assay (Figs. 5 and 8).

Next, we wanted to examine if a single domain of p53 (DBD) is sufficient to trigger apoptosis or if full length p53 is essential for cell death induction. Although the TD was reported to be essential for *wt* p53 function to exert its apoptotic effect via Bak oligomerization (24), we note our important discovery, that the DBD in isolation with a MTS from Bak or Bax is sufficient to induce apoptosis (Fig. 7). Murphy and colleagues reported that p53 must form a dimer or a tetramer for initiating Bak oligomerization (24). However, our data is consistent with our previous finding (27) and other reports (10,11) that monomeric p53 or just the DBD is sufficient to trigger mitochondrial dependent apoptosis. Moreover, the DBD of p53 (specifically through residues L120, R248, R273, R280, G285 and G287) has been shown to be the domain responsible for binding to Bak (25). An possible explanation to why DBD fused to MTS is sufficient to trigger apoptosis could be that since *wt* p53 does not have a MTS, mitochondrial import of *wt* p53 is only possible through dimerization and monoubiquitination via MDM2 (6). We postulate that forcing the DBD of p53 to be in close proximity to Bak via the Bak targeting signal may trigger an interaction with Bak via the previously reported residues in the DBD region leading to activation of the apoptotic pathway (25). In *wt* p53 the lack of a Bak MTS does not allow the interaction to take place. These results suggest that the Bak MTS fused to DBD can replace MBD and TD for mitochondrial import and is sufficient to cause Bak homo-oligomerization and apoptosis.

To ensure that this finding is not a T47D cell specific effect, we tested the DBD-BakMTS and DBD-BaxMTS in three different cancer cell lines (Fig. 8). In fact, DBD-BakMTS showed even significantly higher (Fig. 8a) or trending higher (Figs. 7a and 8c and e) activity compared to p53-BakMTS. A possible reason for the higher activity of DBD-BakMTS over full length p53-BakMTS is that DBD-BakMTS is lacking the MBD and C-terminus which are essential for the p53 degradation pathway. MDM2 binds to MBD of p53 and initiates polyubiquitination of the C-terminus causing proteasomal degradation (42,43). As DBD-BakMTS lacks the MBD and C-terminus, it may avoid polyubiquitination and subsequent proteasomal degradation, thus making it more stable than p53-BakMTS.

Unlike constructs fused to Bak MTS, Bax tagged constructs showed inconsistent apoptotic activity profiles (Figs. 7 and 8). In SKOV-3, p53-BaxMTS and DBD-BaxMTS activities were not significantly different from their negative control E-BaxMTS (Fig. 8d), and in H1373 p53-BaxMTS did not show higher activity than E-BaxMTS (Fig. 8b). A possible explanation for this is that Bax is constantly shuttled between cytoplasm and mitochondria (Fig. 3) (44,45) . Mitochondrial p53 might lack the ability to activate cytoplasmic Bax while the fraction of Bax which is present at the mitochondria might not be sufficient to induce apoptosis in certain cell lines. This might offer an explanation why p53-BaxMTS and DBD-BaxMTS show inconsistent results (Figs. 7a and 8b, d and f). Unlike Bax, Bak is mainly present at the mitochondria and sequestered by anti-apoptotic Mcl-1 and to a certain extent by Bcl-XL (19).

As our ultimate goal is to find a construct capable of robust apoptosis, we proceeded with BakMTS constructs for further studies. The apoptotic mechanism of p53-BakMTS and DBD-BakMTS was then investigated. p53-BakMTS causes apoptosis through a p53/Bak specific pathway, which was confirmed by mutating amino acids of p53 DBD (K120, R248, R273, R280, E285, E287) that are known to interact with the pro-apoptotic Bak protein to abolish any p53/Bak specific interactions (25). In fact, mutating these amino acids showed a complete loss of p53-BakMTS and DBD-BakMTS function (Fig. 9a).

Besides pro-apoptotic Bak, p53 also interacts with anti-apoptotic Bcl-XL through its DBD (residues G117, S121, C176, H178, N239, M243, R248, G279, and R280) (10). p53 interacts through amino acids R248 and R280 with Bak and Bax. To further validate that the apoptotic mechanism is mainly dependent on pro-apoptotic Bak protein and not Bcl-XL, the p53K120E-BakMTS and DBDK120E-BakMTS were created. This K120 residue is known to be significant

and specific for the p53/Bak interaction (25). K120E mutation in p53-BakMTS and DBD-BakMTS resulted in dramatic loss of activity suggesting involvement of Bak/specific p53 pathway (Fig. 9b).

Our mitochondrially targeted p53 could potentially have additive or synergistic apoptotic effects with endogenous *wt* p53. *wt* p53 mainly translocates to the nucleus and triggers transactivation of genes responsible for the extrinsic and intrinsic pathway. While mitochondrial p53 might trigger the first wave of intrinsic apoptosis, *wt* p53 might additively or synergically enhance apoptosis via activation of the extrinsic and intrinsic pathway. This situation would occur only if endogenous *wt* p53 was activated under stress conditions such as radiation or chemotherapy treatment.

CONCLUSION

In summary, our data shows that fusing p53 to MTSs from Bak or Bax results in mitochondrial localization and activation of an intrinsic apoptotic response. DBD-BakMTS and p53-BakMTS show apoptosis in breast, non-small cell lung, ovarian and cervical carcinomas in a p53/Bak dependent manner. Our next step is to test p53-BakMTS and DBD-BakMTS using adenoviral drug delivery in orthotopic breast cancer and ovarian cancer models to validate this *in vitro* work. Ultimately, correction of the p53 pathway and activation of apoptosis may be a universal approach. Mitochondrially targeted p53, which does not dimerize nor activate genes in the nucleus, simply has a direct apoptotic effect. Therefore, functional, mitochondrially targeted monomeric p53 reintroduced into cancer cells would act as a "sledgehammer," effective under any circumstances regardless of genetics or the pathway upon which the cancer develops.

ACKNOWLEDGMENTS AND DISCLOSURES

Research reported in this publication was supported by the National Cancer Institute of the National Institutes of Health under award number R01-CA151847. The authors would also like to acknowledge Christian Raab for his technical work. We also would like to thank Ben Bruno and Geoff Miller for reviewing the manuscript. We acknowledge the use of DNA/Peptide Core and Flow Cytometry Core (NCI Cancer Center Support Grant P30 CA042014, Huntsman Cancer Institute).

REFERENCES

1. Haupt S, Berger M, Goldberg Z, Haupt Y. Apoptosis —the p53 network. J Cell Sci. 2003;116(Pt 20):4077–85.
2. Davis JR, Mossalam M, Lim CS. Controlled access of p53 to the nucleus regulates its proteasomal degradation by MDM2. Mol Pharm. 2013;10(4):1340–9.
3. Weinberg RL, Freund SM, Veprintsev DB, Bycroft M, Fersht AR. Regulation of DNA binding of p53 by its C-terminal domain. J Mol Biol. 2004;342(3):801–11.
4. Mihara M, Erster S, Zaika A, Petrenko O, Chittenden T, Pancoska P, *et al.* p53 has a direct apoptogenic role at the mitochondria. Mol Cell. 2003;11(3):577–90.
5. Shaulsky G, Goldfinger N, Ben-Ze'ev A, Rotter V. Nuclear accumulation of p53 protein is mediated by several nuclear localization signals and plays a role in tumorigenesis. Mol Cell Biol. 1990; 10(12):6565–77.
6. Marchenko ND, Wolff S, Erster S, Becker K, Moll UM. Monoubiquitylation promotes mitochondrial p53 translocation. EMBO J. 2007;26(4):923–34.
7. Perfettini JL, Kroemer RT, Kroemer G. Fatal liaisons of p53 with Bax and Bak. Nat Cell Biol. 2004;6(5):386–8.
8. Chipuk JE, Kuwana T, Bouchier-Hayes L, Droin NM, Newmeyer DD, Schuler M, *et al.* Direct activation of Bax by p53 mediates mitochondrial membrane permeabilization and apoptosis. Science. 2004;303(5660):1010–4.
9. Leu JI, Dumont P, Hafey M, Murphy ME, George DL. Mitochondrial p53 activates Bak and causes disruption of a Bak-Mcl1 complex. Nat Cell Biol. 2004;6(5):443–50.
10. Hagn F, Klein C, Demmer O, Marchenko N, Vaseva A, Moll UM, *et al.* BclxL changes conformation upon binding to wild-type but not mutant p53 DNA binding domain. J Biol Chem. 2010;285(5):3439–50.
11. Tomita Y, Marchenko N, Erster S, Nemajerova A, Dehner A, Klein C, *et al.* WT p53, but not tumor-derived mutants, bind to Bcl2 via the DNA binding domain and induce mitochondrial permeabilization. J Biol Chem. 2006;281(13):8600–6.
12. Chipuk JE, Fisher JC, Dillon CP, Kriwacki RW, Kuwana T, Green DR. Mechanism of apoptosis induction by inhibition of the anti-apoptotic BCL-2 proteins. Proc Natl Acad Sci U S A. 2008;105(51): 20327–32.
13. Tait SW, Green DR. Mitochondria and cell death: outer membrane permeabilization and beyond. Nat Rev Mol Cell Biol. 2010;11(9): 621–32.
14. Chowdhury I, Tharakan B, Bhat GK. Caspases —an update. Comp Biochem Physiol B Biochem Mol Biol. 2008;151(1):10–27.
15. Minn AJ, Rudin CM, Boise LH, Thompson CB. Expression of bcl-xL can confer a multidrug resistance phenotype. Blood. 1995;86(5): 1903–10.
16. Yoshino T, Shiina H, Urakami S, Kikuno N, Yoneda T, Shigeno K, *et al.* Bcl-2 expression as a predictive marker of hormone-refractory prostate cancer treated with taxane-based chemotherapy. Clin Cancer Res. 2006;12(20 Pt 1):6116–24.
17. Green DR, Walczak H. Apoptosis therapy: driving cancers down the road to ruin. Nat Med. 2013;19(2):131–3.
18. Kang MH, Reynolds CP. Bcl-2 inhibitors: targeting mitochondrial apoptotic pathways in cancer therapy. Clin Cancer Res. 2009;15(4): 1126–32.
19. Willis SN, Chen L, Dewson G, Wei A, Naik E, Fletcher JI, *et al.* Proapoptotic Bak is sequestered by Mcl-1 and Bcl-xL, but not Bcl-2, until displaced by BH3-only proteins. Genes Dev. 2005;19(11):1294–305.
20. Ku B, Liang C, Jung JU, Oh BH. Evidence that inhibition of BAX activation by BCL-2 involves its tight and preferential interaction with the BH3 domain of BAX. Cell Res. 2011;21(4):627–41.
21. Schinzel A, Kaufmann T, Schuler M, Martinalbo J, Grubb D, Borner C. Conformational control of Bax localization and apoptotic activity by Pro168. J Cell Biol. 2004;164(7):1021–32.
22. Ferrer PE, Frederick P, Gulbis JM, Dewson G, Kluck RM. Translocation of a Bak C-terminus mutant from cytosol to mitochondria

to mediate cytochrome C release: implications for Bak and Bax apoptotic function. PLoS One. 2012;7(3):e31510.
23. Nechushtan A, Smith CL, Hsu YT, Youle RJ. Conformation of the Bax C-terminus regulates subcellular location and cell death. EMBO J. 1999;18(9):2330–41.
24. Pietsch EC, Leu JI, Frank A, Dumont P, George DL, Murphy ME. The tetramerization domain of p53 is required for efficient BAK oligomerization. Cancer Biol Ther. 2007;6(10):1576–83.
25. Pietsch EC, Perchiniak E, Canutescu AA, Wang G, Dunbrack RL, Murphy ME. Oligomerization of BAK by p53 utilizes conserved residues of the p53 DNA binding domain. J Biol Chem. 2008; 283(30):21294–304.
26. Mossalam M, Matissek KJ, Okal A, Constance JE, Lim CS. Direct induction of apoptosis using an optimal mitochondrially targeted p53. Mol Pharm. 2012;9(5):1449–58.
27. Matissek KJ, Mossalam M, Okal A, Lim CS. The DNA binding domain of p53 is sufficient to trigger a potent apoptotic response at the mitochondria. Mol Pharm. 2013;10:3592–602.
28. Constance JE, Woessner DW, Matissek KJ, Mossalam M, Lim CS. Enhanced and selective killing of chronic myelogenous leukemia cells with an engineered BCR-ABL binding protein and imatinib. Mol Pharm. 2012;9(11):3318–29.
29. Costes SV, Daelemans D, Cho EH, Dobbin Z, Pavlakis G, Lockett S. Automatic and quantitative measurement of protein-protein colocalization in live cells. Biophys J. 2004;86(6):3993–4003.
30. Bolte S, Cordelieres FP. A guided tour into subcellular colocalization analysis in light microscopy. J Microsc. 2006;224(Pt 3):213–32.
31. Okal A, Mossalam M, Matissek KJ, Dixon AS, Moos PJ, Lim CS. A chimeric p53 evades mutant p53 transdominant inhibition in cancer cells. Mol Pharm. 2013;10:3922–33.
32. Schmid I, Krall WJ, Uittenbogaart CH, Braun J, Giorgi JV. Dead cell discrimination with 7-amino-actinomycin D in combination with dual color immunofluorescence in single laser flow cytometry. Cytometry. 1992;13(2):204–8.
33. Yahagi N, Shimano H, Matsuzaka T, Najima Y, Sekiya M, Nakagawa Y, *et al.* p53 Activation in adipocytes of obese mice. J Biol Chem. 2003;278(28):25395–400.
34. Wurstle ML, Laussmann MA, Rehm M. The central role of initiator caspase-9 in apoptosis signal transduction and the regulation of its activation and activity on the apoptosome. Exp Cell Res. 2012; 318(11):1213–20.
35. Darzynkiewicz Z, Bruno S, Del Bino G, Gorczyca W, Hotz MA, Lassota P, *et al.* Features of apoptotic cells measured by flow cytometry. Cytometry. 1992;13(8):795–808.
36. Yin Q, Park HH, Chung JY, Lin SC, Lo YC, da Graca LS, *et al.* Caspase-9 holoenzyme is a specific and optimal procaspase-3 processing machine. Mol Cell. 2006;22(2):259–68.
37. Nigro JM, Baker SJ, Preisinger AC, Jessup JM, Hostetter R, Cleary K, *et al.* Mutations in the p53 gene occur in diverse human tumour types. Nature. 1989;342(6250):705–8.
38. Bodner SM, Minna JD, Jensen SM, D'Amico D, Carbone D, Mitsudomi T, *et al.* Expression of mutant p53 proteins in lung cancer correlates with the class of p53 gene mutation. Oncogene. 1992;7(4): 743–9.
39. Yaginuma Y, Westphal H. Abnormal structure and expression of the p53 gene in human ovarian carcinoma cell lines. Cancer Res. 1992;52(15):4196–9.
40. Goodrum FD, Ornelles DA. p53 status does not determine outcome of E1B 55-kilodalton mutant adenovirus lytic infection. J Virol. 1998;72(12):9479–90.
41. Erster S, Moll UM. Stress-induced p53 runs a direct mitochondrial death program: its role in physiologic and pathophysiologic stress responses in vivo. Cell Cycle. 2004;3(12):1492–5.
42. Nalepa G, Rolfe M, Harper JW. Drug discovery in the ubiquitin-proteasome system. Nat Rev Drug Discov. 2006;5(7):596–613.
43. Haupt Y, Maya R, Kazaz A, Oren M. Mdm2 promotes the rapid degradation of p53. Nature. 1997;387(6630):296–9.
44. Schellenberg B, Wang P, Keeble JA, Rodriguez-Enriquez R, Walker S, Owens TW, *et al.* Bax exists in a dynamic equilibrium between the cytosol and mitochondria to control apoptotic priming. Mol Cell. 2013;49(5):959–71.
45. Edlich F, Banerjee S, Suzuki M, Cleland MM, Arnoult D, Wang C, *et al.* Bcl-x(L) retrotranslocates Bax from the mitochondria into the cytosol. Cell. 2011;145(1):104–16.